
# Photoelectron spectroscopy of a series of acetate and propionate esters

Małgorzata A. Śmiałek, Julien Guthmuller, Michael A. MacDonald, Lucia Zuin, Jacques Delwiche, Marie-Jeanne Hubin-Franskin, Tadeusz Lesniewski, Nigel J. Mason, Paulo Limão-Vieira

PII: S0022-4073(17)30397-7
DOI: 10.1016/j.jqsrt.2017.06.018
Reference: JQSRT 5745

To appear in: *Journal of Quantitative Spectroscopy & Radiative Transfer*

Received date: 21 May 2017
Revised date: 14 June 2017
Accepted date: 15 June 2017

Please cite this article as: Małgorzata A. Śmiałek, Julien Guthmuller, Michael A. MacDonald, Lucia Zuin, Jacques Delwiche, Marie-Jeanne Hubin-Franskin, Tadeusz Lesniewski, Nigel J. Mason, Paulo Limão-Vieira, Photoelectron spectroscopy of a series of acetate and propionate esters, *Journal of Quantitative Spectroscopy & Radiative Transfer* (2017), doi: 10.1016/j.jqsrt.2017.06.018

**Highlights**

- Presents the valence shell structure and the PE for acetate and propionate esters
- Data obtained through VUV PES and ab initio calculations
- The most distinctive vibrational transition is a C=O stretch combined with a C-O stretch
- Ionization energy depends on the size of the molecule, not much on its conformation

# Photoelectron spectroscopy of a series of acetate and propionate esters

Małgorzata A. Śmiałek[a,b,*], Julien Guthmuller[c], Michael A. MacDonald[d], Lucia Zuin[d], Jacques Delwiche[e], Marie-Jeanne Hubin-Franskin[e], Tadeusz Lesniewski[f], Nigel J. Mason[b], Paulo Limão-Vieira[g]

[a] *Department of Control and Power Engineering, Faculty of Ocean Engineering and Ship Technology, Gdańsk University of Technology, Gabriela Narutowicza 11/12, 80-233 Gdańsk, Poland*
[b] *School of Physical Sciences, The Open University, Walton Hall, Milton Keynes, MK7 6AA, United Kingdom*
[c] *Department of Theoretical Physics and Quantum Information, Faculty of Applied Physics and Mathematics, Gdańsk University of Technology, Gabriela Narutowicza 11/12, 80-233 Gdańsk, Poland*
[d] *Canadian Light Source Inc., 44 Innovation Boulevard, Saskatoon SK S7N 2V3, Canada*
[e] *Département de Chimie, Université de Liège, Institut de Chimie-Bât. B6C, B-4000 Liège, Belgium*
[f] *Institute of Experimental Physics, Faculty of Mathematics, Physics and Informatics, University of Gdańsk, 80-308 Gdańsk, Poland*
[g] *Laboratório de Colisões Atómicas e Moleculares, CEFITEC, Departamento de Física, Faculdade de Ciências e Tecnologia, Universidade NOVA de Lisboa, 2829-516 Caparica, Portugal*

**Abstract**

The electronic state and photoionization spectroscopy of a series of acetate esters: methyl acetate, isopropyl acetate, butyl acetate and pentyl acetate as well as two propionates: methyl propionate and ethyl propionate, have been determined using vacuum-ultraviolet photoelectron spectroscopy. These experimental investigations are complemented by *ab initio* calculations. The measured first adiabatic and vertical ionization energies were determined as: 10.21 and 10.45 eV for methyl acetate, 9.99 and 10.22 eV for isopropyl acetate, 10.07 and 10.26 eV for butyl acetate, 10.01 and 10.22 eV for pentyl acetate, 10.16 and 10.36 eV for methyl propionate and 9.99 and 10.18 eV for ethyl propionate. For the four smaller esters vibrational transitions were calculated and compared with those identified in the photoelectron spectrum, revealing the most distinctive ones to be a C−O stretch combined with a C=O stretch. The ionization energies of methyl and ethyl esters as well as for a series of formates and acetates were compared showing a clear dependence of the value of the ionization energy on the size of the molecule with very little influence of its conformation.

*Keywords:* Photoelectron spectroscopy, esters, *ab initio* calculations

## 1. Introduction

Esters are emitted to the atmosphere both through anthropogenic and natural [1] sources. In industry they play an important role, among others, as solvents [2] and in use of fragrances and flavourings, while recently they have also become a significant additive in biodiesel fuels [3]. Esters are also of astrochemical interest, since it has been shown that small esters are present in the interstellar space [4].

In order to assess the role of such compounds in atmospheric and interstellar chemistry, it is necessary to acquire an accurate kinetic chemistry data including their reactions in the gas phase as well as detailed information on their electronic structure and properties, such as their ionization energies (IEs). TThe electronic state and

*Corresponding author
*Email address:* smialek@pg.gda.pl (Małgorzata A. Śmiałek )

photoionization spectroscopy of those esters that have a high vapour pressure can be obtained by the use of VUV photoelectron energy analysis assisted by the state-of -the-art *ab initio* calculations.

In this paper we provided a detailed photoelectron spectroscopy (PES) analysis of the series of acetate and propionate esters: methyl acetate, isopropyl acetate, butyl acetate, pentyl acetate, methyl propionate and ethyl propionate. Electronic excitation of these compounds have been described with aid of quantum chemistry calculations. Combining our findings with data obtained for those esters that have been studied previously: methyl formate [5], ethyl formate [6], isobutyl formate [7], isobutyl acetate [8], ethyl acetate [9], methyl butyrate and methyl valerate [10] we can draw some conclusions on the influence of the increase in the alkyl and aryl group on the ionization energy of ester molecules.

## 2. Experimental Section

### *2.1. Ester samples*

The liquid samples used both in He(I) and synchrotron PES experiments were purchased from Sigma-Aldrich, all with a purity better than 99 %. The samples were degassed by repeated freeze–pump–thaw cycles with no further purification of the samples.

### *2.2. Photoelectron spectra measurements*

The He(I) (21.22 eV) photoelectron spectra of methyl acetate, pentyl acetate, methyl propionate and ethyl propionate (Figures 3 and 5) were measured at the Université de Liège, Belgium. The apparatus has also been described in detail previously [11]. Briefly, it consists of a 180° hemispherical electrostatic analyser with a mean radius of 5 cm, the analyser is used in the constant pass energy mode. The incident photons are produced by a d.c. discharge in a two-stage differentially pumped helium lamp. The energy scale is calibrated using the $X^2\Sigma_g^+$, $\nu' = 0$ and $A^2\Pi_u$, $\nu' = 0$ peaks of $N_2^+$, rounded to three decimal places [12, 13]. The resolution of the present spectrum is 40 meV and the accuracy of the energy scale is estimated to be ± 2 meV. The photoelectron spectra presented here are the sum of at least 70 individual spectra. This procedure allows a good signal-to-noise ratio while keeping the pressure in the spectrometer low ($< 5 \times 10^{-6}$ mbar).

The photoelectron spectra of isopropyl acetate and butyl acetate (Figure 3) were measured at the VLS-PGM beamline[14] at the Canadian Light Source facility in Saskatoon, Canada, using a Double Toroidal Coincidence Spectrometer, described previously [15]. Although designed and primarly used for analysis of Noble gases and small, diatomic molecules it has been successfully applied to measurements of more complicated systems such as pyrimidine and its heavier derivatives [16] or other esters [7]. Briefly, a photoelectron-photoelectron coincidence spectrometer has been developed in which two electrons, of specified energies, are detected over a wide range of emission angles. The spectrometer is based on a toroidal geometry and has properties ideally suited for measuring electron angle distributions since toroidal analysers can be made to energy select the photoelectrons while preserving the initial angle of emission. The spectrometer consists of two toroidal analyzers, each focused on the interaction region. One collects electrons over an azimuthal range of 180°, the other over 120°. The electrostatic analyzers are independent, i.e. they are able to detect dissimilar electron energies albeit with different resolutions. Both analyzers were set at a pass energy of 4 eV. In these experiments we have used the data collected by the 180°

toroidal detector. The measured resolution from the nitrogen calibration spectra was 40 meV. The photoexcitation energy of the photoelectron spectrum presented here was 80 eV, recorded with the entrance and exit slits of the VLS-PGM beamline set at 50 micrometer. The recorded spectra were calibrated against the $X^2\Sigma_g^+$, $\nu' = 0$ and $A^2\Pi_u$, $\nu' = 0$ peaks of $N_2^+$, rounded to three decimal places [12, 13].

### *2.3. Computational methods*

The ground state geometry, harmonic vibrational frequencies, and normal coordinates of the neutral singlet state ($S_0$) and ionic doublet state ($D_0$) of the different esters were obtained with the Gaussian 09 program [17] by means of second-order Møller-Plesset (MP2) calculations [18] in association with the aug-cc-pVTZ basis set. The ionic state was described by open-shell unrestricted calculations. The first ionization energies (IE) were computed from the energy difference between the neutral and ionic ground states. The vertical IE was calculated at the ground state geometry of the neutral compound and the adiabatic IE was evaluated using the optimized geometries of the neutral and ionic ground states. Additionally, the first IE was calculated with the coupled-cluster singles and doubles (CCSD), and the coupled-cluster singles, doubles and perturbative triples (CCSD(T)) methods [19, 20] using the aug-cc-pVTZ basis set and employing the optimized geometries at the MP2/aug-cc-pVTZ level of approximation. Furthermore, the zero point vibrational energy (ZPVE) correction to the adiabatic IEs was determined from the MP2/aug-cc-pVTZ harmonic vibrational frequencies. This correction was also applied to the values calculated with the CCSD and CCSD(T) methods. Higher IEs were obtained with the Partial Third Order (P3) and Outer Valence Greens Function (OVGF) propagator methods [21] using the aug-cc-pVTZ basis set and the MP2/aug-cc-pVTZ geometry. The Franck-Condon (FC) factors, associated with the first photoelectron band, were calculated using recursive relations and include Duschinsky rotation effects [22, 23, 24, 25]. These calculations made use of the ground state geometries, harmonic frequencies and normal coordinates calculated with the MP2/aug-cc-pVTZ method for the neutral ($S_0$ state) and ionic ($D_0$ state) forms of the esters.

## 3. Results and Discussion

### *3.1. Structure and Properties of Acetates and Propionates*

The molecular structure of acetate esters is presented in Figure 1 (1-4a). In all cases, in accord with previous studies of formate [5, 6, 7] and acetate [9, 8] esters, the highest occupied molecular orbital (HOMO) in the neutral ground state is localized largely on the terminal oxygen in-plane lone pair ($n_{O1}$), as seen in Figure 1 (1-4b). For methyl acetate the HOMO is $(16a')^2$, for isopropyl acetate – $(20a')^2$, for butyl acetate – $(25a')^2$, and for pentyl acetate – $(28a')^2$.

Analogously, in the propionate esters, methyl and ethyl, Figure 2 (1a and 2a), the HOMO is also localised in the neutral ground state on the terminal oxygen in-plane lone pair ($n_{O1}$, Figure 2(1b and 2b)). For methyl propionate the HOMO is $(19a')^2$, whilst for ethyl propionate it is $(22a')^2$.

Theoretical calculations have determined the ground-state full electron configuration of core and valence orbitals for all the investigated acetate and propionate esters and these are listed in Table 1.

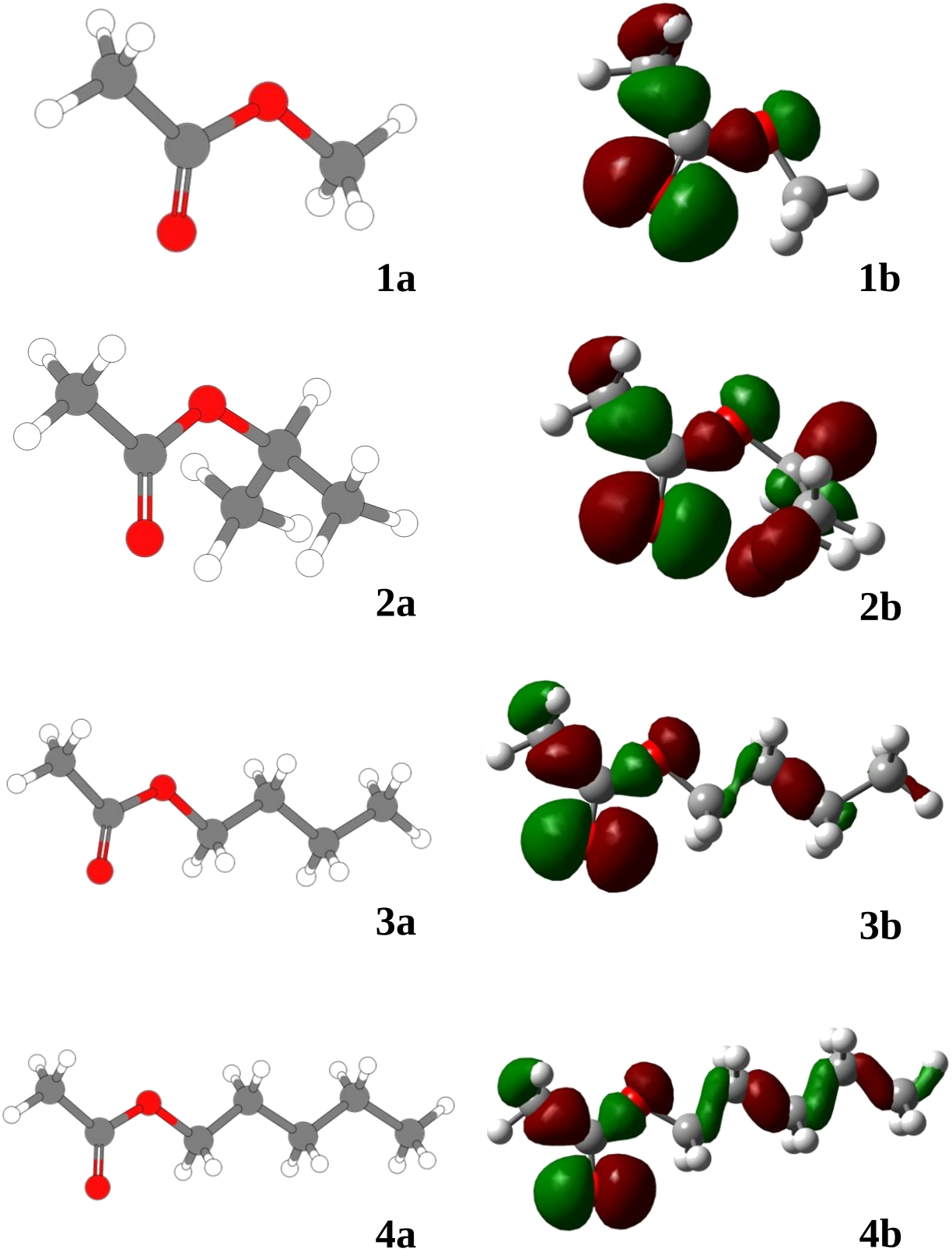


Figure 1: Structure (a) and HOMO orbitals (b) of 1: methyl acetate, 2: isopropyl acetate, 3: butyl acetate and 4: pentyl acetate.

| Ester | Core orbitals | Valence orbitals |
|---|---|---|
| Methyl Acetate | $(1a')^2$, $(2a')^2$, $(3a')^2$, $(4a')^2$, $(5a')^2$ | $(6a')^2$, $(7a')^2$, $(8a')^2$, $(9a')^2$, $(10a')^2$, $(11a')^2$, $(1a'')^2$, $(12a')^2$, $(2a'')^2$, $(13a')^2$, $(14a')^2$, $(15a')^2$, $(3a'')^2$, $(4a'')^2$, $(16a')^2$ |
| Isopropyl Acetate | $(1a')^2$, $(2a')^2$, $(3a')^2$, $(4a')^2$, $(5a')^2$, $(1a'')^2$, $(6a')^2$ | $(7a')^2$, $(8a')^2$, $(9a')^2$, $(10a')^2$, $(2a'')^2$, $(11a')^2$, $(12a')^2$, $(13a')^2$, $(14a')^2$, $(3a'')^2$, $(15a')^2$, $(4a'')^2$, $(16a')^2$, $(17a')^2$, $(5a'')^2$, $(6a'')^2$, $(18a')^2$, $(7a'')^2$, $(19a')^2$, $(8a'')^2$, $(20a')^2$ |
| Butyl Acetate | $(1a')^2$, $(2a')^2$, $(3a')^2$, $(4a')^2$, $(5a')^2$, $(6a')^2$, $(7a')^2$, $(8a')^2$ | $(9a')^2$, $(10a')^2$, $(11a')^2$, $(12a')^2$, $(13a')^2$, $(14a')^2$, $(15a')^2$, $(16a')^2$, $(1a'')^2$, $(17a')^2$, $(18a')^2$, $(2a'')^2$, $(19a')^2$, $(3a'')^2$, $(20a')^2$, $(21a')^2$, $(4a'')^2$, $(22a')^2$, $(5a'')^2$, $(23a')^2$, $(24a')^2$, $(6a'')^2$, $(7a'')^2$, $(25a')^2$ |
| Pentyl Acetate | $(1a')^2$, $(2a')^2$, $(3a')^2$, $(4a')^2$, $(5a')^2$, $(6a')^2$, $(7a')^2$, $(8a')^2$, $(9a')^2$ | $(10a')^2$, $(11a')^2$, $(12a')^2$, $(13a')^2$, $(14a')^2$, $(15a')^2$, $(16a')^2$, $(17a')^2$, $(18a')^2$, $(1a'')^2$, $(19a')^2$, $(20a')^2$, $(2a'')^2$, $(3a'')^2$, $(21a')^2$, $(22a')^2$, $(4a'')^2$, $(23a')^2$, $(24a')^2$, $(5a'')^2$, $(25a')^2$, $(6a'')^2$, $(26a')^2$, $(7a'')^2$, $(27a')^2$, $(8a'')^2$, $(28a')^2$ |
| Methyl Propionate | $(1a')^2$, $(2a')^2$, $(3a')^2$, $(4a')^2$, $(5a')^2$, $(6a')^2$ | $(7a')^2$, $(8a')^2$, $(9a')^2$, $(10a')^2$, $(11a')^2$, $(12a')^2$, $(13a')^2$, $(1a'')^2$, $(14a')^2$, $(2a'')^2$, $(15a')^2$, $(3a'')^2$, $(16a')^2$, $(17a')^2$, $(18a')^2$, $(4a'')^2$, $(5a'')^2$, $(19a')^2$ |
| Ethyl Propionate | $(1a')^2$, $(2a')^2$, $(3a')^2$, $(4a')^2$, $(5a')^2$, $(6a')^2$, $(7a')^2$ | $(8a')^2$, $(9a')^2$, $(10a')^2$, $(11a')^2$, $(12a')^2$, $(13a')^2$, $(14a')^2$, $(15a')^2$, $(1a'')^2$, $(16a')^2$, $(2a'')^2$, $(17a')^2$, $(3a'')^2$, $(18a')^2$, $(19a')^2$, $(20a')^2$, $(4a'')^2$, $(21a')^2$, $(5a'')^2$, $(6a'')^2$, $(22a')^2$ |

Table 1: Ground-state electron configurations of acetate and propionate esters, showing the core and valence molecular orbitals.

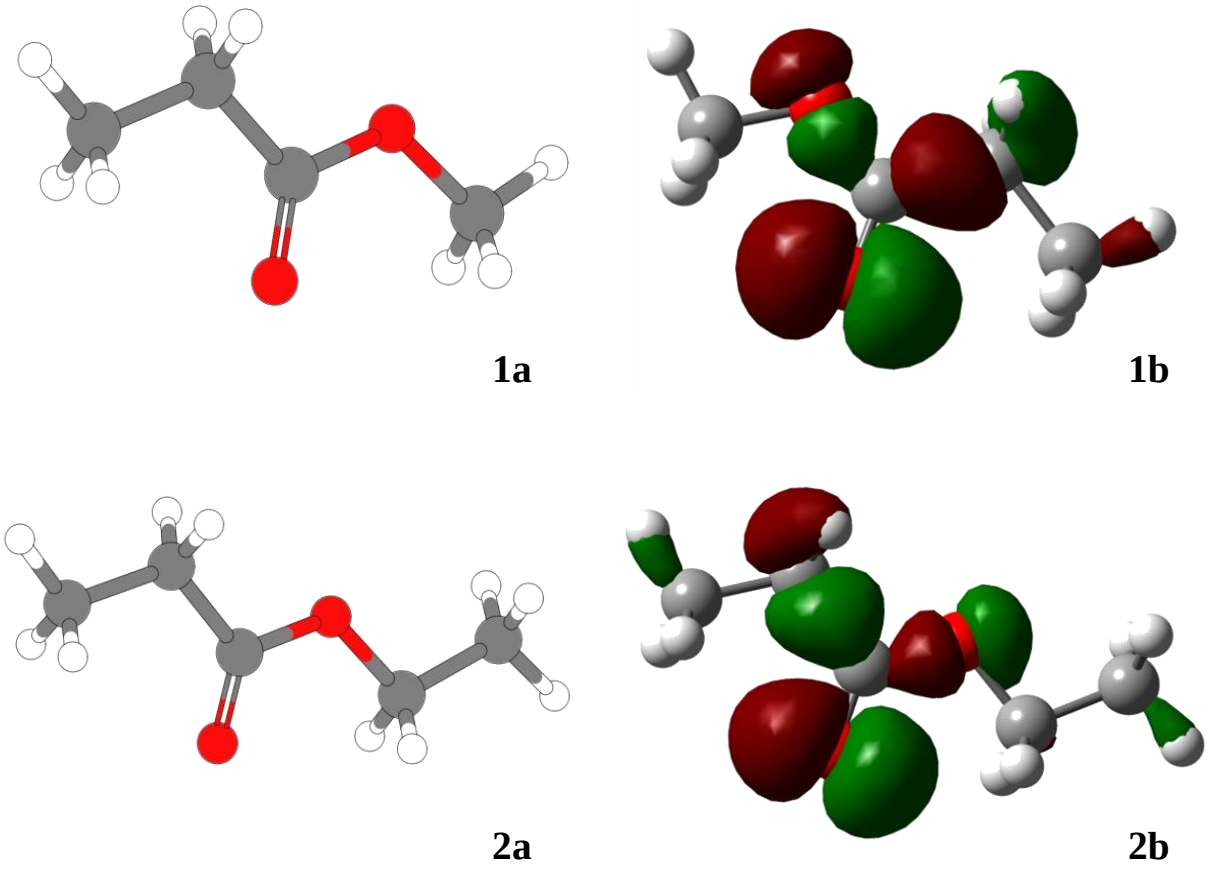


Figure 2: Structure (a) and HOMO orbitals (b) of 1: methyl propionate, 2: ethyl propionate.

*3.2. Photoelectron Spectra of Acetates*

Figure 3 presents photoelectron spectra of methyl, isopropyl, butyl and pentyl acetate. In most cases the two bands that originate from ionization from the HOMO and the HOMO-1 are separated from other higher lying, overlapping bands. It was possible to derive values for most of the electronic states predicted by the computations, the obtained values are presented in Tables 2 and 3 where they are compared with computed derived values.

Vertical and adiabatic ionization energies of methyl acetate were determined experimentally to be 10.45 and 10.21 eV, respectively. For the first state, $16a'^{-1}$, these values agree very well with computed ones at the CCSD(T) level, yielding 10.554 and 10.184 eV, respectively, as well as with the adiabatic values derived in previous experimental studies 10.27 eV [26], 10.33 eV (with vertical value 10.48 eV) [27] and 10.25 eV [28]. A very good agreement for the $4a''^{-1}$ state has been obtained between the value obtained in this work, 11.183 eV, for the vertical transition and the computed value of 11.510 eV (at P3 level), as well as a previously published value of 11.16 eV [27]. In the measured photoelectron spectrum it was also possible, with assistance of calculations, to determine the energies of transitions from higher MOs that have not been established previously. The values derived from the experimental spectrum are in a good agreement with the ones calculated at the OVGF level and are listed in Table 2. The respective positions of consequent IEs are marked with black (vertical) and red (adiabatic) bars in the measured spectrum of methyl acetate in Figure 3.

The isopropyl acetate photoelectron spectrum has been measured at the synchrotron radiation source and extends to 28 eV. The first vertical and adiabatic ionization energies from the $20a'^{-1}$ state were found at 10.22 and 9.99 eV and are in a good agreement with the ones calculated at CCSD(T) level, yielding 10.132 and 9.781 eV, respectively. They are also in a good agreement with values measured previously for the adiabatic transition at 9.99 eV [26] and at 10.08 eV (with the vertical transition at 10.38 eV)[27]. For the transition from $8a''^{-1}$, a measured value of 10.78 eV agrees well with both the calculated at P3 (11.065 eV) and OVGF (11.087 eV) levels and with the one reported previously, 10.77 eV [27]. It was also possible to assign IEs from higher MOs, based on the computations. The highest energies visible in the experimental spectrum were assigned purely based on the order of higher MO and should be treated some caution. All the calculated and measured values are listed in Table 2 and marked in Figure 3.

The vertical value of the $25a'^{-1}$ transition measured for butyl acetate, 10.26 eV, is in reasonable agreement with the one obtained from calculations at P3 level, 10.575 eV. The adiabatic value for this transition was only determined through measurements and yielded 10.07 eV, being in a good agreement with the one from the literature, 10.01 eV [26]. The IEs from higher MOs were determined based on calculations, however as some values overlapped, it was not possible to make unambiguous assignments. All the values are collected in Table 3 and also marked in Figure 3.

The ionization energy of pentyl acetate has not been determined previously. Here we have determined experimental values for the first vertical and adiabatic ionization energies of 10.22 and 10.01 eV, respectively. As in case of other large ester molecules, the computed values were higher than the ones obtained from measurements and yielded at best 10.584 eV, when calculated at P3 level. The newly obtained values are summarized in Table 3 and marked in Figure 3.

For the smaller esters, methyl and isopropyl acetate, it was also possible to calculate the vibronic structure of

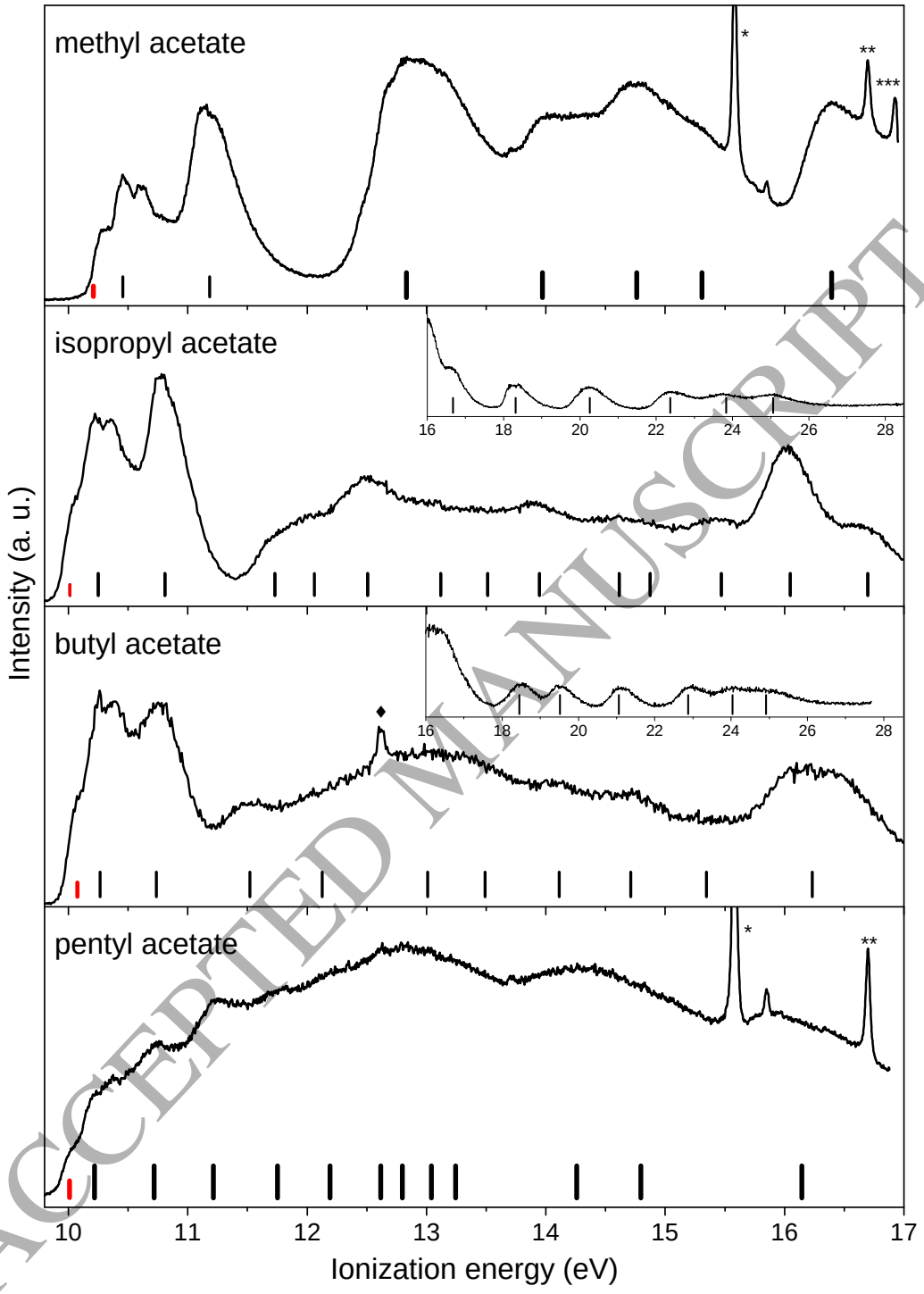


Figure 3: Photoelectron spectra of methyl acetate $C_3H_6O_2$, isopropyl acetate $C_5H_{10}O_2$, butyl acetate $C_6H_{12}O_2$ and pentyl acetate $C_7H_{14}O_2$ in the 9.7–17 eV region; methyl and pentyl acetate are He(I) spectra, whereas isopropyl and butyl acetate spectra were measured on the synchrotron light source and extend to 28 eV (see insets). Red lines mark adiabatic transitions, black lines - vertical transitions (*$N_2^+$ $X^2\Sigma_g^+$, $v$' = 0 produced by the He(I)$\alpha$ line; **$N_2^+$ $X^2\Sigma_g^+$, $v$' = 1 produced by the He(I)$\alpha$ line; ***$N_2^+$ $A^2\Pi_u$, $v$' = 0 produced by the He(I) $\alpha$ line; ♦ $^2B_1$ $H_2O$ contamination).

| Configuration | Calculated | | | | | Experimental / eV |
|---|---|---|---|---|---|---|
| | P3 | OVGF | MP2 | CCSD | CCSD(T) | |
| **Methyl acetate** | | | | | | |
| $^2$A' (16a'$^{-1}$) | 10.749 | 10.937 | 10.973/10.549 | 10.477/10.078 | 10.554/10.184 | 10.45/10.21 |
| $^2$A" (4a"$^{-1}$) | 11.510 | 11.593 | - | - | - | 11.18 |
| $^2$A" (3a"$^{-1}$) | 13.344 | 13.392 | - | - | - | 13.12 |
| $^2$A' (15a'$^{-1}$) | 13.214 | 13.336 | - | - | - | 12.83 |
| $^2$A' (14a'$^{-1}$) | 14.300 | 14.259 | - | - | - | 13.97 |
| $^2$A' (13a'$^{-1}$) | 14.940 | 15.016 | - | - | - | 14.76 |
| $^2$A" (2a"$^{-1}$) | 15.301 | 15.31 | - | - | - | 15.31 |
| $^2$A' (12a'$^{-1}$) | 16.721 | 16.687 | - | - | - | 16.40 |
| $^2$A" (1a"$^{-1}$) | 16.791 | 16.769 | - | - | - | - |
| $^2$A' (11a'$^{-1}$) | 17.161 | 17.119 | - | - | - | - |
| **Isopropyl acetate** | | | | | | |
| $^2$A' (20a'$^{-1}$) | 10.348 | 10.522 | 10.601/10.164 | 10.082/9.688 | 10.132/9.781 | 10.22/9.99 |
| $^2$A" (8a"$^{-1}$) | 11.065 | 11.087 | - | - | - | 10.78 |
| $^2$A' (19a'$^{-1}$) | 12.171 | 12.222 | - | - | - | 11.70 |
| $^2$A" (7a"$^{-1}$) | 12.564 | 12.605 | - | - | - | 12.03 |
| $^2$A' (18a'$^{-1}$) | 12.884 | 13.030 | - | - | - | 12.48 |
| $^2$A" (6a"$^{-1}$) | 13.309 | 13.425 | - | - | - | 13.09 |
| $^2$A" (5a"$^{-1}$) | 14.012 | 14.143 | - | - | - | 13.48 |
| $^2$A' (17a'$^{-1}$) | 14.398 | 14.454 | - | - | - | 13.92 |
| $^2$A' (16a'$^{-1}$) | 14.722 | 14.831 | - | - | - | 14.59 |
| $^2$A" (4a"$^{-1}$) | 14.861 | 14.893 | - | - | - | 14.84 |
| $^2$A' (15a'$^{-1}$) | 15.310 | 15.251 | - | - | - | 15.44 |
| $^2$A" (3a"$^{-1}$) | 16.155 | 16.107 | - | - | - | 16.02 |
| $^2$A' (14a'$^{-1}$) | 16.496 | 16.481 | - | - | - | 16.67 |
| $^2$A' (13a'$^{-1}$) | 16.949 | 16.937 | - | - | - | 18.31 |
| $^2$A' (12a'$^{-1}$) | 17.968 | 18.042 | - | - | - | 20.25 |
| $^2$A' (11a'$^{-1}$) | - | - | - | - | - | 22.36 |
| $^2$A" (2a"$^{-1}$) | - | - | - | - | - | 23.83 |
| $^2$A' (10a'$^{-1}$) | - | - | - | - | - | 25.06 |

Table 2: Calculated vertical/adiabatic ionization energies of methyl acetate and isopropyl acetate at the MP2/aug-cc-pVTZ geometry, compared with experimental values, all in eV. Adiabatic ionization energies include ZPVE correction of -0.032 eV for methyl acetate and -0.040 eV for isopropyl acetate.

| Configuration | Calculated | | Experimental / eV |
|---|---|---|---|
| | P3 | OVGF | |
| **Butyl acetate** | | | |
| $^2$A' ($25a'^{-1}$) | 10.575 | 10.746 | 10.26/10.07 |
| $^2$A" ($7a"^{-1}$) | 11.227 | 11.341 | 10.73 |
| $^2$A" ($6a"^{-1}$) | 12.085 | 12.242 | 11.52(*) |
| $^2$A' ($24a'^{-1}$) | 12.048 | 12.020 | 11.52(*) |
| $^2$A' ($23a'^{-1}$) | 12.270 | 12.349 | 12.12 |
| $^2$A" ($5a"^{-1}$) | 12.802 | 12.910 | 13.01 |
| $^2$A' ($22a'^{-1}$) | 12.943 | 13.019 | 13.49 |
| $^2$A" ($4a"^{-1}$) | 13.704 | 13.803 | 14.11 |
| $^2$A' ($21a'^{-1}$) | 14.144 | 14.145 | 14.71 |
| $^2$A' ($20a'^{-1}$) | 14.446 | 14.527 | 15.34 |
| $^2$A" ($3a"^{-1}$) | 15.116 | 15.104 | 16.23(*) |
| $^2$A' ($19a'^{-1}$) | 14.934 | 15.025 | 16.23(*) |
| $^2$A" ($2a"^{-1}$) | 16.017 | 16.033 | 18.50 |
| $^2$A' ($18a'^{-1}$) | 16.332 | 16.288 | 19.58 |
| $^2$A' ($17a'^{-1}$) | 16.835 | 16.826 | 21.12 |
| $^2$A" ($1a"^{-1}$) | 16.989 | 17.037 | 22.93 |
| $^2$A' ($16a'^{-1}$) | - | - | 24.09 |
| $^2$A' ($15a'^{-1}$) | - | - | 24.97 |
| **Pentyl acetate** | | | |
| $^2$A' ($28a'^{-1}$) | 10.584 | 10.728 | 10.22/10.01 |
| $^2$A" ($8a"^{-1}$) | 11.207 | 11.324 | 10.72 |
| $^2$A' ($27a'^{-1}$) | 11.625 | 11.622 | 11.21 |
| $^2$A" ($7a"^{-1}$) | 11.922 | 12.094 | 11.75 |
| $^2$A' ($26a'^{-1}$) | 12.040 | 12.076 | 12.19 |
| $^2$A" ($6a"^{-1}$) | 12.402 | 12.540 | 12.62 |
| $^2$A' ($25a'^{-1}$) | 12.646 | 12.746 | 12.80 |
| $^2$A" ($5a"^{-1}$) | 13.178 | 13.279 | 13.04 |
| $^2$A' ($24a'^{-1}$) | 13.420 | 13.506 | 13.24 |
| $^2$A' ($23a'^{-1}$) | 14.124 | 14.100 | 14.26 |
| $^2$A" ($4a"^{-1}$) | 14.231 | 14.340 | 14.80 |
| $^2$A' ($22a'^{-1}$) | 14.635 | 14.692 | - |
| $^2$A' ($21a'^{-1}$) | 14.851 | 14.967 | - |
| $^2$A" ($3a"^{-1}$) | 15.387 | 15.385 | 16.15 |
| $^2$A" ($2a"^{-1}$) | 16.175 | 16.213 | - |
| $^2$A' ($20a'^{-1}$) | 16.281 | 16.238 | - |
| $^2$A' ($19a'^{-1}$) | 16.823 | 16.817 | - |
| $^2$A" ($1a"^{-1}$) | 16.985 | 17.040 | - |

Table 3: Calculated vertical/adiabatic ionization energies of butyl acetate and pentyl acetate at the MP2/aug-cc-pVTZ geometry, compared with experimental values, all in eV; (*) – ambiguous assignment.

the first band of the photoelectron spectrum. In Figure 4, the low energy part of the photoelectron spectrum with resolved HOMO and HOMO-1 states (solid lines) for acetate esters is presented and for methyl and isopropyl acetate these data are compared with calculated spectra obtained using the Franck–Condon (FC) factors (dashed lines). Both the experimental and computed spectra revealed possible vibronic structure that for methyl and isopropyl acetate was assigned based on the values of calculated vibrational transitions, whereas for butyl acetate and pentyl acetate this was ascribed based on our results previously obtained for other ester molecules.

The vibrational transitions calculated for methyl acetate and isopropyl acetate are shown in Table 4, together with corresponding FC factors. From this analysis it was possible to assign the main vibronic structure visible in the $16a'^{-1}$ state of methyl acetate to the $\nu_{21}$ mode that designates combined C−O and C=O stretches with an experimentally determined spacing of c.a. 0.177 eV, also marked in Figure 4. The computed value for this mode in the ground state of the neutral is 0.194 eV. This structure is then accompanied by combination bands involving mainly the $\nu_5$ mode that, according to our calculations, corresponds to OCC deformation combined with CO stretch and $CH_3$ rocking and can be labelled as the OCC out-of-plane bend [29] and is derived from the spectrum to be approximately 0.050 eV, which agrees well with computed value of 0.043 eV. A similar assignment shown in both Table 4 and Figure 4, has been obtained for isopropyl acetate where, in the HOMO $20a'^{-1}$ state, a combination of $\nu_{35}$ that corresponds also to combined C−O and C=O stretches is observed and experimentally derived value for this mode is 0.179 eV, with $\nu_7 + \nu_8$ from the OCC out-of-plane bend [29], being c.a. 0.062 eV. Computed values of these modes yield 0.192 eV and 0.081 eV, respectively, and are also in a good agreement with the experimental findings.

For the larger butyl and pentyl acetates it was only possible to resolve the most prominent vibronic structure seen in the experimental spectrum, presented in Figure 4. For butyl acetate it was denoted as $\nu_A$=0.163 eV, whereas for pentyl acetate it was denoted as $\nu_B$=0.170 eV and in both cases these are, based on previous analysis of other esters, ascribed to combined C−O and C=O stretches, based on previous analysis of other esters.

### *3.3. Photoelectron spectra of Propionates*

Figure 5 presents photoelectron spectra of methyl and ethyl propionate. The two bands that originate from ionization from HOMO and HOMO-1 are separated from the remaining, overlapping bands of higher states. It was possible to identify values for most of the electronic states predicted by the computations, the values obtained are presented in Tables 5 and marked in Figure 5 with red (adiabatic) and black (vertical) bars.

Experimental investigations revealed that the vertical and adiabatic ionization energies for the transition from $19a'^{-1}$ state of methyl propionate yield 10.36 and 10.16 eV, respectively and these are in a good agreement with the values calculated at the CCSD(T) level (10.445 and 10.099 eV, respectively). The measured adiabatic value agrees very well with the only one found in the literature, 10.15 eV [26]. The measured values of IEs from higher MOs have been assigned based on the calculations performed at the OVGF level and are in a good agreement with the computed ones.

Similarly the values for vertical and adiabatic transitions obtained for ionization from HOMO $22a'^{-1}$ of ethyl propionate, 10.18 and 9.99 eV, respectively, are in a good agreement with computational calculations at the CCSD and CCSD(T) level and the previously reported adiabatic value of 10.00 eV [26].

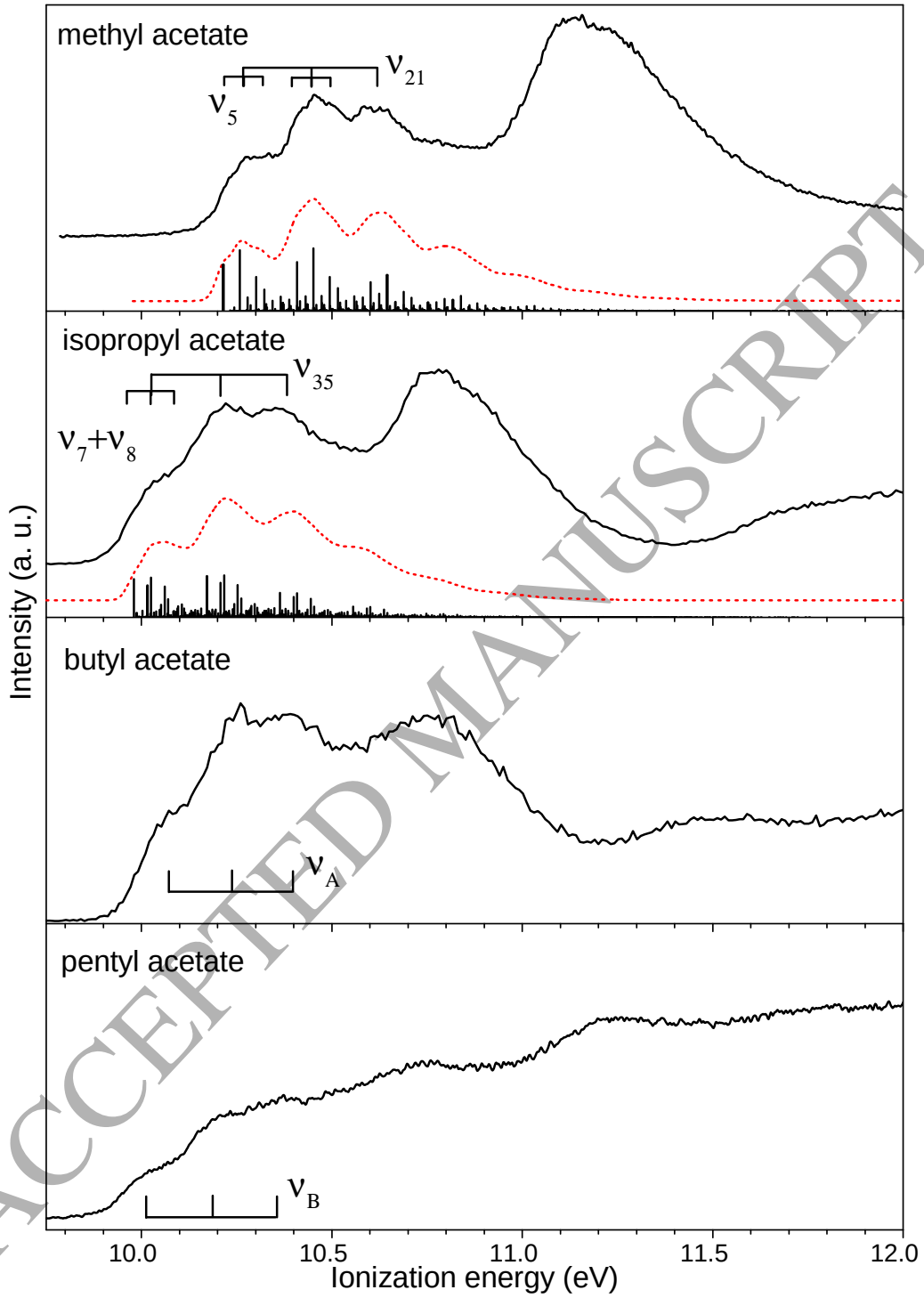


Figure 4: Photoelectron spectra of methyl acetate $C_3H_6O_2$, isopropyl acetate $C_5H_{10}O_2$, butyl acetate $C_6H_{12}O_2$ and pentyl acetate $C_7H_{14}O_2$ in the 9.5–12 eV region with vibronic excitation assignment; dashed red line represents theoretical Franck-Condon vibrational structure based on FC factors (black bars), calculated for the first photoelectron band of methyl and isopropyl acetate.

| Vibrational state | Frequency ($cm^{-1}$) | FC factor |
|---|---|---|
| **Methyl acetate** | | |
| 0-0 | – | 0.0304 |
| $\nu_5$ | 348 | 0.0397 |
| $\nu_6$ | 518 | 0.0091 |
| $2\nu_5$ | 695 | 0.0222 |
| $\nu_5 + \nu_6$ | 866 | 0.0141 |
| $\nu_{21}$ | 1561 | 0.0321 |
| $\nu_{21} + \nu_5$ | 1908 | 0.0411 |
| $\nu_{21} + \nu_6$ | 2079 | 0.0099 |
| $\nu_{21} + 2\nu_5$ | 2256 | 0.0225 |
| $\nu_{21} + \nu_5 + \nu_6$ | 2427 | 0.0150 |
| $2\nu_{21}$ | 3122 | 0.0188 |
| $2\nu_{21} + \nu_5$ | 3469 | 0.0236 |
| $2\nu_{21} + \nu_6$ | 3640 | 0.0059 |
| $2\nu_{21} + 2\nu_5$ | 4158 | 0.0005 |
| $2\nu_{21} + \nu_5 + \nu_6$ | 3988 | 0.0088 |
| $3\nu_{21}$ | 4683 | 0.0080 |
| $3\nu_{21} + \nu_5$ | 5030 | 0.0099 |
| $3\nu_{21} + \nu_6$ | 5201 | 0.0026 |
| $3\nu_{21} + 2\nu_5$ | 5378 | 0.0052 |
| $3\nu_{21} + \nu_5 + \nu_6$ | 5548 | 0.0038 |
| **Isopropyl acetate** | | |
| 0-0 | – | 0.0150 |
| $\nu_7$ | 289 | 0.0125 |
| $\nu_8$ | 363 | 0.0156 |
| $\nu_7 + \nu_8$ | 652 | 0.0121 |
| $2\nu_8$ | 725 | 0.0072 |
| $\nu_{35}$ | 1549 | 0.0162 |
| $\nu_{35} + \nu_7$ | 1838 | 0.0135 |
| $\nu_{35} + \nu_8$ | 1911 | 0.0164 |
| $\nu_{35} + \nu_7 + \nu_8$ | 2200 | 0.0127 |
| $\nu_{35} + 2\nu_8$ | 2274 | 0.0074 |
| $2\nu_{35}$ | 3097 | 0.0097 |
| $2\nu_{35} + \nu_7$ | 3386 | 0.0080 |
| $2\nu_{35} + \nu_8$ | 3460 | 0.0095 |
| $2\nu_{35} + \nu_7 + \nu_8$ | 3749 | 0.0074 |
| $2\nu_{35} + 2\nu_8$ | 3822 | 0.0042 |
| $3\nu_{35}$ | 4645 | 0.0042 |
| $3\nu_{35} + \nu_7$ | 4935 | 0.0035 |
| $3\nu_{35} + \nu_8$ | 5008 | 0.0040 |
| $3\nu_{35} + \nu_7 + \nu_8$ | 5297 | 0.0031 |
| $3\nu_{35} + 2\nu_8$ | 5371 | 0.0017 |

Table 4: Main vibrational transitions and Franck-Condon (FC) factors contributing to the vibrational structure of the first photoelectron band for methyl and isopropyl acetate (MP2/aug-cc-pVTZ).

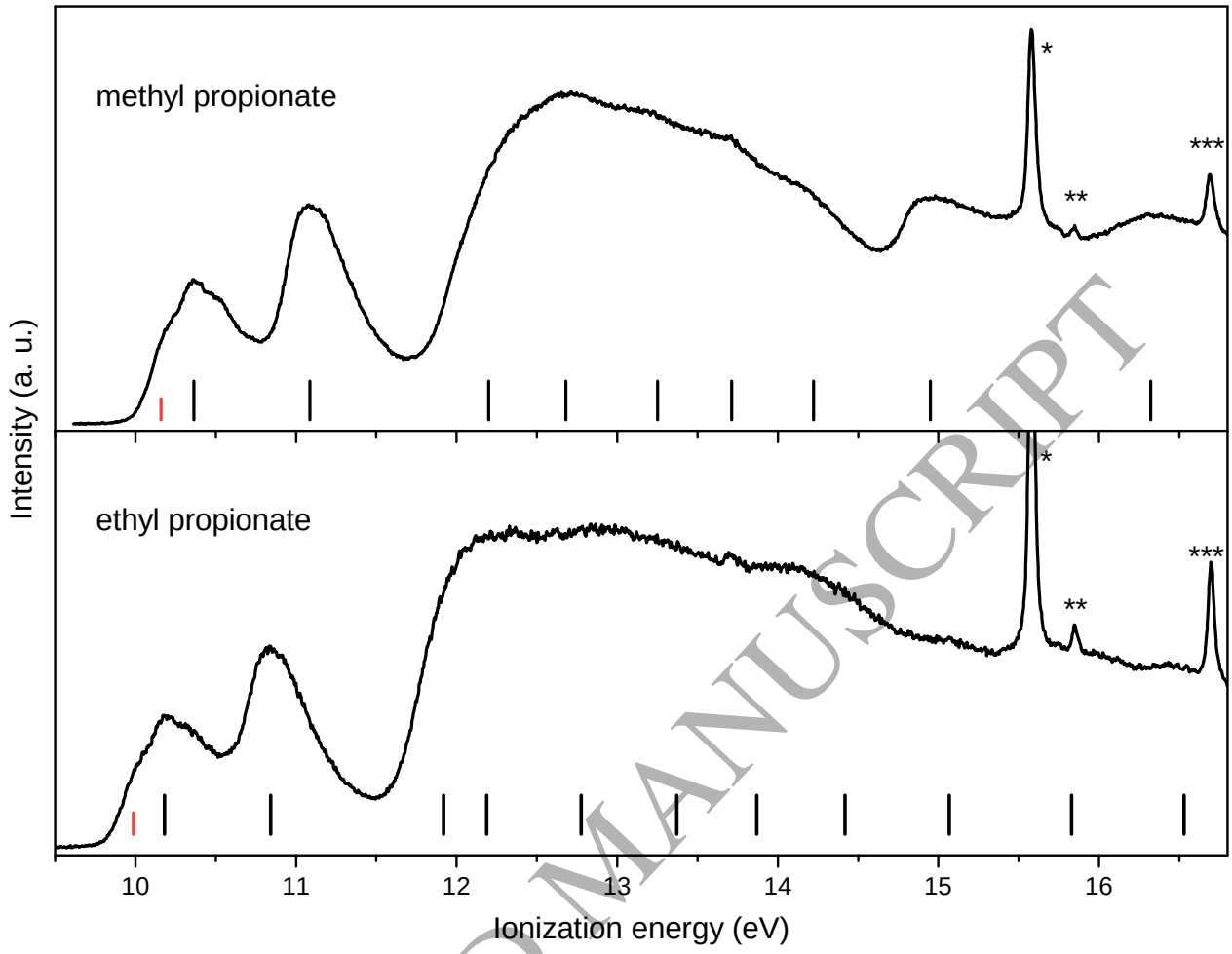


Figure 5: He(I) photoelectron spectra of methyl propionate $C_4H_8O_2$ and ethyl propionate $C_5H_{10}O_2$ in the 9.5–16.75 eV region. Red lines mark adiabatic transitions, black lines - vertical transitions (*$N_2^+$ $X^2\Sigma_g^+$, $v$' = 0 produced by the He(I)$\alpha$ line; **$N_2^+$ $X^2\Sigma_g^+$, $v$' = 1 produced by the He(I)$\alpha$ line; ***$N_2^+$ $A^2\Pi_u$, $v$' = 0 produced by the He(I) $\alpha$ line).

It was also possible to calculate the vibronic structure of the first band of the photoelectron spectrum. In Figure 6, a low energy part of the photoelectron spectrum with resolved HOMO and HOMO-1 states (solid lines) for propionate esters is presented and compared with the calculated spectrum obtained from the Franck–Condon factors (dashed lines). Both the experimental and computed spectra revealed possible vibronic structure that has been assigned based on the values of calculated vibrational transitions, shown in Table 6, together with corresponding FC factors. From this analysis it was possible to assign the main vibronic structure, visible in the $19a'^{-1}$ state of methyl propionate to the $\nu_{28}$ mode that designates combined C−O and C=O stretches with an experimentally determined spacing of c.a. 0.194 eV. A similar assignment has been obtained for ethyl propionate where, in the HOMO $22a'^{-1}$ state, a combination of $\nu_{35}$ was resolved that also corresponds to combined C−O and C=O stretches and the experimentally derived value for this mode yields 0.183 eV. Both values agree well with computed ones that yield 0.191 eV for $\nu_{28}$ in methyl propionate and 0.190 eV for $\nu_{35}$ in ethyl propionate.

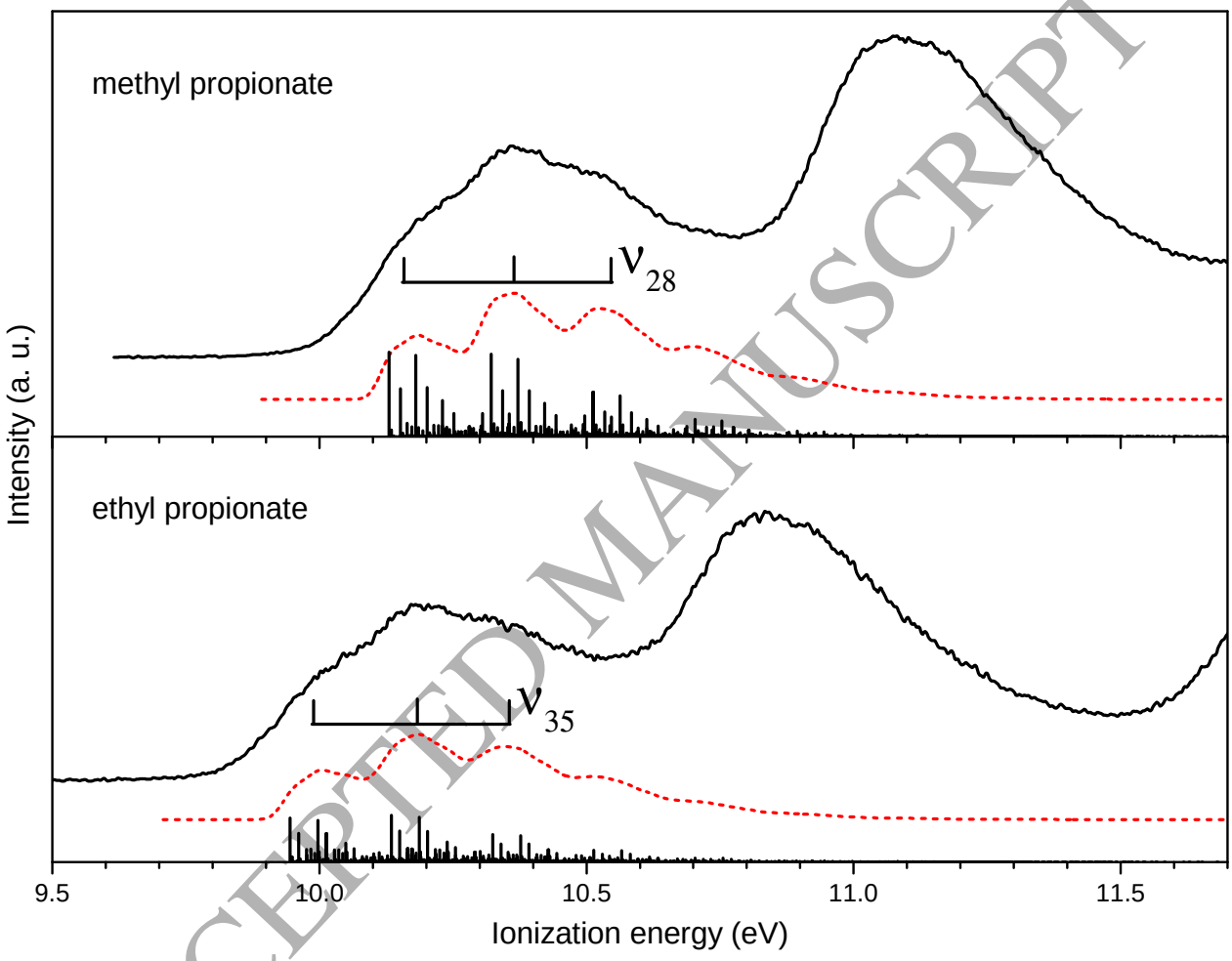


Figure 6: Photoelectron spectra of methyl propionate $C_4H_8O_2$ and ethyl propionate $C_5H_{10}O_2$ in the 9.5–11.7 eV region with vibronic excitation assignment; dashed red line represents theoretical Franck-Condon vibrational structure based on FC factors (black bars), calculated for the first photoelectron band of methyl and ethyl propionate.

| Configuration | Calculated | | | | | Experimental / eV |
|---|---|---|---|---|---|---|
| | P3 | OVGF | MP2 | CCSD | CCSD(T) | |
| **Methyl propionate** | | | | | | |
| $^2$A' (19a'$^{-1}$) | 10.658 | 10.817 | 10.883/10.472 | 10.368/9.992 | 10.445/10.099 | 10.36/10.16 |
| $^2$A" (5a"$^{-1}$) | 11.410 | 11.503 | - | - | - | 11.09 |
| $^2$A" (4a"$^{-1}$) | 12.686 | 12.722 | - | - | - | 12.20 |
| $^2$A' (18a'$^{-1}$) | 12.982 | 13.060 | - | - | - | 12.68 |
| $^2$A' (17a'$^{-1}$) | 13.310 | 13.174 | - | - | - | 13.25 |
| $^2$A' (16a'$^{-1}$) | 13.510 | 13.643 | - | - | - | 13.71 |
| $^2$A" (3a"$^{-1}$) | 13.804 | 13.895 | - | - | - | 14.22 |
| $^2$A' (15a'$^{-1}$) | 15.123 | 15.084 | - | - | - | 14.95 |
| $^2$A" (2a"$^{-1}$) | 15.737 | 15.719 | - | - | - | - |
| $^2$A' (14a'$^{-1}$) | 16.497 | 16.469 | - | - | - | 16.32 |
| $^2$A" (1a"$^{-1}$) | 16.821 | 16.804 | - | - | - | - |
| $^2$A' (13a'$^{-1}$) | 17.254 | 17.227 | - | - | - | - |
| $^2$A' (12a'$^{-1}$) | 18.835 | 18.869 | - | - | - | - |
| **Ethyl propionate** | | | | | | |
| $^2$A' (22a'$^{-1}$) | 10.531 | 10.692 | 10.742/10.310 | 10.228/9.833 | 10.301/9.936 | 10.18/9.99 |
| $^2$A" (6a"$^{-1}$) | 11.227 | 11.334 | - | - | - | 10.84 |
| $^2$A" (5a"$^{-1}$) | 12.546 | 12.603 | - | - | - | 11.92 |
| $^2$A' (21a'$^{-1}$) | 12.674 | 12.750 | - | - | - | 12.19 |
| $^2$A" (4a"$^{-1}$) | 13.097 | 13.201 | - | - | - | 12.77 |
| $^2$A' (20a'$^{-1}$) | 13.119 | 13.002 | - | - | - | - |
| $^2$A' (19a'$^{-1}$) | 13.214 | 13.277 | - | - | - | 13.37 |
| $^2$A' (18a'$^{-1}$) | 14.243 | 14.346 | - | - | - | - |
| $^2$A" (3a"$^{-1}$) | 14.335 | 14.458 | - | - | - | 14.42 |
| $^2$A' (17a'$^{-1}$) | 14.497 | 14.606 | - | - | - | - |
| $^2$A" (2a"$^{-1}$) | 15.991 | 15.981 | - | - | - | 15.07 |
| $^2$A' (16a'$^{-1}$) | 16.229 | 16.213 | - | - | - | 15.83 |
| $^2$A" (1a"$^{-1}$) | 16.924 | 16.942 | - | - | - | - |
| $^2$A" (15a'$^{-1}$) | 17.073 | 17.053 | - | - | - | 16.53 |
| $^2$A' (14a'$^{-1}$) | 18.852 | 18.895 | - | - | - | - |

Table 5: Calculated vertical/adiabatic ionization energies of methyl and ethyl propionate at the MP2/aug-cc-pVTZ geometry, compared with experimental values, all in eV. Adiabatic ionization energies include ZPVE correction of -0.035 eV for methyl propionate and -0.037 eV for ethyl propionate.

| Vibrational state | Frequency ($cm^{-1}$) | FC factor |
|---|---|---|
| **Methyl propionate** | | |
| 0-0 | – | 0.0264 |
| $\nu_4$ | 173 | 0.0150 |
| $\nu_7$ | 404 | 0.0255 |
| $\nu_4+\nu_7$ | 577 | 0.0154 |
| $2\nu_7$ | 808 | 0.0113 |
| $\nu_{28}$ | 1541 | 0.0259 |
| $\nu_{28}+\nu_4$ | 1714 | 0.0145 |
| $\nu_{28}+\nu_7$ | 1945 | 0.0243 |
| $\nu_{28}+\nu_4+\nu_7$ | 2118 | 0.0144 |
| $\nu_{28}+2\nu_7$ | 2350 | 0.0105 |
| $2\nu_{28}$ | 3082 | 0.0140 |
| $2\nu_{28}+\nu_4$ | 3255 | 0.0077 |
| $2\nu_{28}+\nu_7$ | 3487 | 0.0128 |
| $2\nu_{28}+\nu_4+\nu_7$ | 3660 | 0.0075 |
| $2\nu_{28}+2\nu_7$ | 3891 | 0.0054 |
| $3\nu_{28}$ | 4624 | 0.0055 |
| $3\nu_{28}+\nu_4$ | 4797 | 0.0030 |
| $3\nu_{28}+\nu_7$ | 5028 | 0.0049 |
| $3\nu_{28}+\nu_4+\nu_7$ | 5201 | 0.0028 |
| $3\nu_{28}+2\nu_7$ | 5432 | 0.0020 |
| **Ethyl propionate** | | |
| 0-0 | – | 0.0155 |
| $\nu_3$ | 127 | 0.0102 |
| $\nu_9$ | 421 | 0.0146 |
| $\nu_3+\nu_9$ | 547 | 0.0100 |
| $2\nu_9$ | 841 | 0.0066 |
| $\nu_{35}$ | 1529 | 0.0165 |
| $\nu_{35}+\nu_3$ | 1656 | 0.0009 |
| $\nu_{35}+\nu_9$ | 1950 | 0.0157 |
| $\nu_{35}+\nu_3+\nu_9$ | 2076 | 0.0108 |
| $\nu_{35}+2\nu_9$ | 2370 | 0.0071 |
| $2\nu_{35}$ | 3058 | 0.0097 |
| $2\nu_{35}+\nu_3$ | 3185 | 0.0064 |
| $2\nu_{35}+\nu_9$ | 3478 | 0.0093 |
| $2\nu_{35}+\nu_3+\nu_9$ | 3605 | 0.0064 |
| $2\nu_{35}+2\nu_9$ | 3899 | 0.0042 |
| $3\nu_{35}$ | 4587 | 0.0042 |
| $3\nu_{35}+\nu_3$ | 4713 | 0.0028 |
| $3\nu_{35}+\nu_9$ | 5007 | 0.0040 |
| $3\nu_{35}+\nu_3+\nu_9$ | 5134 | 0.0027 |
| $3\nu_{35}+2\nu_9$ | 5428 | 0.0018 |

Table 6: Main vibrational transitions and Franck-Condon (FC) factors contributing to the vibrational structure of the first photoelectron band for methyl and ethyl propionate (MP2/aug-cc-pVTZ).

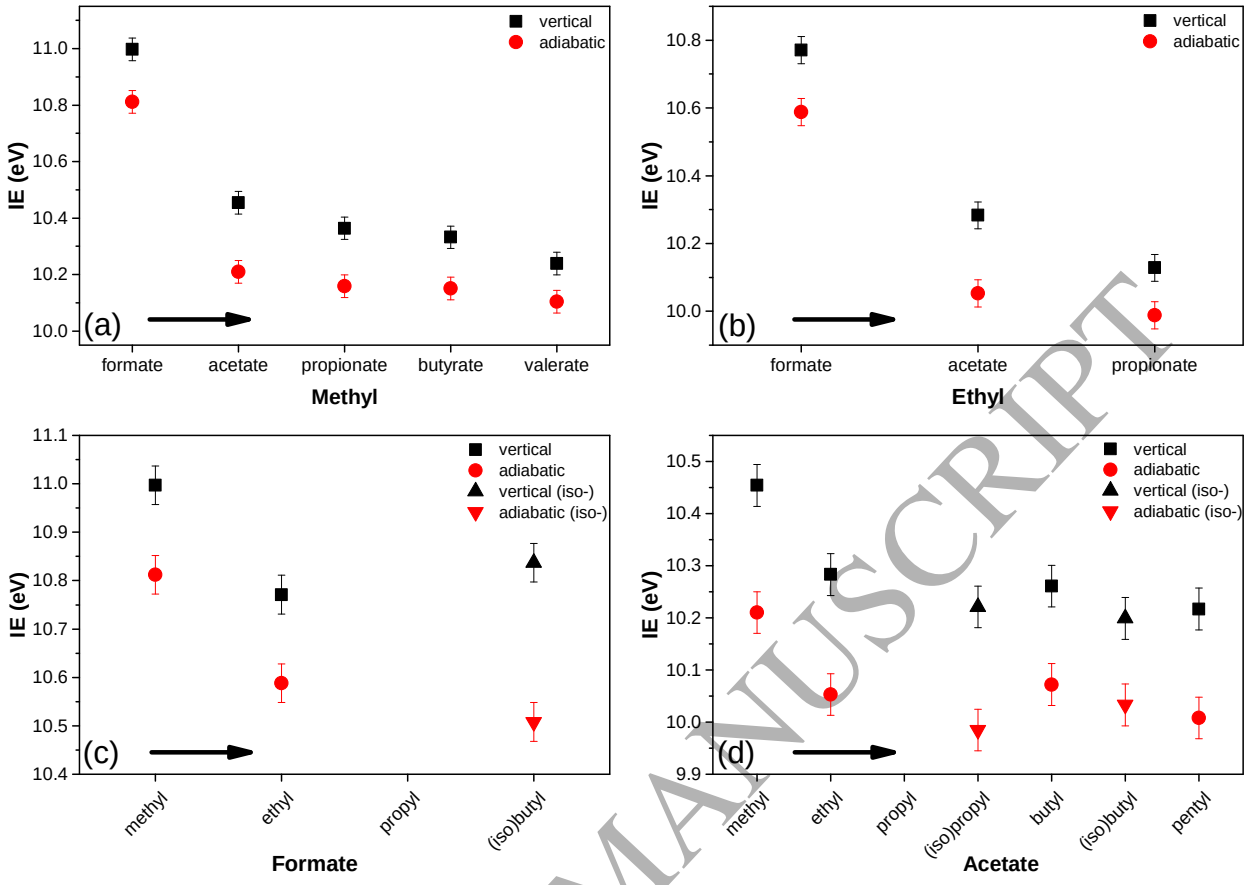


Figure 7: Comparison between the experimental values of vertical (black) and adiabatic (red) first photoionization energies of series of (a) methyl and (b) ethyl esters, as well as (c) formates and (d) acetates; arrows mark the increase in the size of the aryl (a, b) and alkyl (c, d) group; the error bars represent the FWHM of the calibration lines in the spectra of ∼40 meV.

### *3.4. Vertical and adiabatic photoionization energies of series of esters.*

Based on the collected spectra of series of esters it was possible to correlate the values of adiabatic and vertical $n_0$ photoionization energies of methyl and ethyl esters with an increase of the length of the aryl group, as well as obtaining a similar correlation in the formate and acetate esters with respect to the length of the alkyl group. The results of these correlations are shown in Figure 7, presenting the relations for (a) methyl esters, (b) ethyl esters, (c) formates and (d) acetates. In this figure, the vertical transitions are marked in black and the adiabatic ones are labelled red. The triangular symbols mark the energies obtained for the *iso*-conformers. It is interesting to note that an identical mode description on the lowest-lying ionic state of propionic acid has been observed previously [30].

In all cases the IEs decrease with an increase of the size of the molecule, nonetheless, the differences observed in the decrease in the IEs values is much more distinctive when the aryl group is enlarged rather than the alkyl one. Also, the case of ethyl formate and methyl acetate shows that for the increase in IE, the aryl group is responsible for. This assumption is also supported by the results obtained for the *iso*-conformers of acetates, where the variation in the value of IE is not significant within the assigned experimental uncertainty.

## 4. Conclusions

This paper presents a detailed analysis of photoelectron spectra of methyl, isopropyl, butyl and pentyl acetate as well as methyl and ethyl propionate esters, supported by *ab initio* calculations. For the first time the core and valence shell structure has been resolved for all these compounds and the first vertical and adiabatic ionization energies have been determined and compared to those available from the literature.

The vertical and adiabatic IEs were combined with those obtained previously for other ester molecules and cross-examined against the size of the alkyl and aryl group size in the ester molecule. It was shown that the increase in both the groups decreases the IE, although the influence of the aryl group is more prominent than of the alkyl one. The *iso*-conformation has very little effect on the values if IE.

## 5. Acknowledgment

M.A.Ś. acknowledges the visiting fellowship position in the Molecular Physics Group, Open University and a Santander Research and Scholarship award received through the OU. Part of research described in this paper was performed at the Canadian Light Source, which is supported by the Canadian Foundation for Innovation, Natural Sciences and Engineering Research Council of Canada, the University of Saskatchewan, the Government of Saskatchewan, Western Economic Diversification Canada, the National Research Council Canada, and the Canadian Institutes of Health Research. All the calculations described in this paper have been performed at the Academic Center (CI TASK) in Gdańsk and at Universitätsrechenzentrum of the Friedrich-Schiller University in Jena. PLV acknowledges the Portuguese National Funding Agency FCT-MCTES through research grant UID/FIS/00068/2013.

## References

[1] D. Helmig, J. Möller, W. Klein, Volatile organic substances in a forest atmosphere, Chemosphere 19 (8) (1989) 1399 – 1412. doi:http://dx.doi.org/10.1016/0045-6535(89)90088-X.
URL http://www.sciencedirect.com/science/article/pii/004565358990088X

[2] G. V. Buxton, J. Wang, G. A. Salmon, Rate constants for the reactions of $NO_3^{\cdot}$, $SO_4^{\cdot}$ and $Cl^{\cdot}$ radicals with formate and acetate esters in aqueous solution, Phys. Chem. Chem. Phys. 3 (2001) 2618–2621. doi:10.1039/B101932P.
URL http://dx.doi.org/10.1039/B101932P

[3] P. Osswald, U. Struckmeier, T. Kasper, K. Kohse-Hoeinghaus, J. Wang, T. A. Cool, N. Hansen, P. R. Westmoreland, Isomer-specific Fuel Destruction Pathways in Rich Flames of Methyl Acetate and Ethyl Formate and Consequences for the Combustion Chemistry of Esters, Journal of Physical Chemistry A 111 (19) (2007) 4093–4101. doi:{10.1021/jp068337w}.

[4] I. Medvedev, F. C. D. Lucia, E. Herbst, Increased complexity in interstellar chemistry: detection and chemical modeling of ethyl formate and n-propyl cyanide in sagittarius b2(n), Astronomy and Astrophysics 499 (2009) 215 – 232.

[5] Y. Nunes, G. Martins, N. J. Mason, D. Duflot, S. V. Hoffmann, J. Delwiche, M.-J. Hubin-Franskin, P. Limão-Vieira, Electronic state spectroscopy of methyl formate probed by high resolution vuv photoabsorption, He(I) photoelectron spectroscopy and ab initio calculations, Physical Chemistry Chemical Physics 12 (2010) 15734–15743.

[6] M. A. Śmiałek, M. Łabuda, J. Guthmuller, M.-J. Hubin-Franskin, J. Delwiche, D. Duflot, N. J. Mason, S. V. Hoffmann, N. C. Jones, P. Limão-Vieira, Valence and ionic lowest-lying electronic states of ethyl formate as studied by high-resolution vacuum ultraviolet photoabsorption, He(I) photoelectron spectroscopy, and ab initio calculations, The Journal of Chemical Physics 141 (10) (2014) 104311 (1–9).

[7] M. A. Śmiałek, M. Łabuda, J. Guthmuller, S. V. Hoffmann, N. C. Jones, M. A. MacDonald, L. Zuin, N. J. Mason, P. Limão-Vieira, Valence and ionic lowest-lying electronic states of isobutyl formate studied by high-resolution vacuum ultraviolet photoabsorption, photoelectron spectroscopy, and ab initio calculations, The Journal of Physical Chemistry A 119 (32) (2015) 8647–8656, pMID: 26176891. doi:10.1021/acs.jpca.5b06053.

[8] M. A. Śmiałek, M. Łabuda, M.-J. Hubin-Franskin, J. Delwiche, S. V. Hoffmann, N. C. Jones, N. J. Mason, P. Limão-Vieira, Isobutyl acetate: electronic state spectroscopy by high-resolution vacuum ultraviolet photoabsorption, He(I) photoelectron spectroscopy and ab initio calculations, The European Physical Journal D in press. doi:10.1140/epjd/e2017-80071-4.

[9] M. A. Śmiałek, M. Łabuda, J. Guthmuller, M.-J. Hubin-Franskin, J. Delwiche, S. V. Hoffmann, N. C. Jones, N. J. Mason, P. Limão-Vieira, Electronic state spectroscopy by high-resolution vacuum ultraviolet photoabsorption, He(I) photoelectron spectroscopy and ab initio calculations of ethyl acetate, Eur. Phys. J. D 70 (6) (2016) 138. doi:10.1140/epjd/e2016-70239-9.
URL http://dx.doi.org/10.1140/epjd/e2016-70239-9

[10] M. Śmiałek, et al., Electronic structure investigation of methyl butyrate and valerate esters, in preparation.

[11] J. Delwiche, P. Natalis, J. Momigny, J. E. Collin, On the photoelectron spectra of HBr and DBr, Journal of Electron Spectroscopy and Related Phenomena 1 (3) (1972-1973) 219 – 225. doi:DOI:10.1016/0368-2048(72)85012-6.

[12] K. P. Huber, C. Jungen, High-resolution jet absorption study of nitrogen near 800 Å, The Journal of Chemical Physics 92 (2) (1990) 850–861. doi:http://dx.doi.org/10.1063/1.458589.
URL http://scitation.aip.org/content/aip/journal/jcp/92/2/10.1063/1.458589

[13] D. A. Shaw, D. M. P. Holland, M. A. MacDonald, A. Hopkirk, M. A. Hayes, S. M. McSweeney, A study of the absolute photoabsorption cross section and the photionization quantum efficiency of nitrogen from the ionization threshold to 485 Å, Chemical Physics 166 (1992) 379–391. doi:10.1016/0301-0104(92)80097-F.

[14] Y. F. Hu, L. Zuin, G. Wright, R. Igarashi, M. McKibben, T. Wilson, S. Y. Chen, T. Johnson, D. Maxwell, B. W. Yates, T. K. Sham, R. Reininger, Commissioning and performance of the variable line spacing plane

grating monochromator beamline at the canadian light source, Review of Scientific Instruments 78 (8) (2007) –. doi:http://dx.doi.org/10.1063/1.2778613.
URL http://scitation.aip.org/content/aip/journal/rsi/78/8/10.1063/1.2778613

[15] T. Reddish, G. Richmond, G. Bagley, J. Wightman, S. Cvejanovic, Dual toroidal photoelectron spectrometer for investigating photodouble ionization in atoms and molecules, Review of Scientific Instruments 68 (7) (1997) 2685–2692. doi:10.1063/1.1148180.

[16] M. Śmiałek, E. Szymańska, M. MacDonald, L. Zuin, N. Mason, Photoelectron spectroscopy of brominated derivative of pyrimidine: 2-bromopyrimidine, The European Physical Journal Special Topics 222 (9) (2013) 2361–2366. doi:10.1140/epjst/e2013-02017-8.
URL http://dx.doi.org/10.1140/epjst/e2013-02017-8

[17] M. J. Frisch, G. W. Trucks, H. B. Schlegel, G. E. Scuseria, M. A. Robb, J. R. Cheeseman, G. Scalmani, V. Barone, B. Mennucci, G. A. Petersson, H. Nakatsuji, M. Caricato, X. Li, H. P. Hratchian, A. F. Izmaylov, J. Bloino, G. Zheng, J. L. Sonnenberg, M. Hada, M. Ehara, K. Toyota, R. Fukuda, J. Hasegawa, M. Ishida, T. Nakajima, Y. Honda, O. Kitao, H. Nakai, T. Vreven, J. A. Montgomery, Jr., J. E. Peralta, F. Ogliaro, M. Bearpark, J. J. Heyd, E. Brothers, K. N. Kudin, V. N. Staroverov, R. Kobayashi, J. Normand, K. Raghavachari, A. Rendell, J. C. Burant, S. S. Iyengar, J. Tomasi, M. Cossi, N. Rega, J. M. Millam, M. Klene, J. E. Knox, J. B. Cross, V. Bakken, C. Adamo, J. Jaramillo, R. Gomperts, R. E. Stratmann, O. Yazyev, A. J. Austin, R. Cammi, C. Pomelli, J. W. Ochterski, R. L. Martin, K. Morokuma, V. G. Zakrzewski, G. A. Voth, P. Salvador, J. J. Dannenberg, S. Dapprich, A. D. Daniels, . Farkas, J. B. Foresman, J. V. Ortiz, J. Cioslowski, D. J. Fox, Gaussian 09 Revision A.02, gaussian Inc. Wallingford CT 2009.

[18] M. Head-Gordon, T. Head-Gordon, Analytic mp2 frequencies without fifth-order storage. theory and application to bifurcated hydrogen bonds in the water hexamer, Chemical Physics Letters 220 (1) (1994) 122 – 128. doi:http://dx.doi.org/10.1016/0009-2614(94)00116-2.
URL http://www.sciencedirect.com/science/article/pii/0009261494001162

[19] G. D. Purvis III, R. J. Bartlett, A full coupledcluster singles and doubles model: The inclusion of disconnected triples, The Journal of Chemical Physics 76 (4) (1982) 1910–1918. arXiv:http://dx.doi.org/10.1063/1.443164, doi:10.1063/1.443164.
URL http://dx.doi.org/10.1063/1.443164

[20] J. A. Pople, M. Head-Gordon, K. Raghavachari, Quadratic configuration interaction. A general technique for determining electron correlation energies, Journal of Chemical Physics 87 (1987) 5968–5975. doi:10.1063/1.453520.

[21] J. Linderberg, Y. Öhrn, Propagators in Quantum Chemistry, Wiley & Sons, Hoboken, NJ, 2004.

[22] P. T. Ruhoff, Recursion relations for multi-dimensional franck-condon overlap integrals, Chemical Physics 186 (2-3) (1994) 355–374.

[23] M. Łabuda, J. Guthmuller, Theoretical study of the photoelectron spectrum of ethyl formate: Ab initio and density functional theory investigation, European Physical Journal-Special Topics 222 (9) (2013) 2257–2266. doi:10.1140/epjst/e2013-02003-2.

[24] J. Guthmuller, F. Zutterman, B. Champagne, Prediction of vibronic coupling and absorption spectra of dimers from time-dependent density functional theory: The case of a stacked streptocyanine, Journal of Chemical Theory and Computation 4 (12) (2008) 2094–2100. doi:10.1021/ct8003047.

[25] J. Guthmuller, F. Zutterman, B. Champagne, Multimode simulation of dimer absorption spectra from first principles calculations: Application to the 3,4,9,10-perylenetetracarboxylic diimide dimer, Journal of Chemical Physics 131 (15). doi:10.1063/1.3245403.

[26] K. Watanabe, T. Nakayama, J. Mottl, Ionization potentials of some molecules, Journal of Quantitative Spectroscopy and Radiative Transfer 2 (4) (1962) 369 – 382. doi:http://dx.doi.org/10.1016/0022-4073(62)90023-7.
URL http://www.sciencedirect.com/science/article/pii/0022407362900237

[27] D. A. Sweigart, D. W. Turner, Lone pair orbitals and their interactions studied by photoelectron spectroscopy. i. carboxylic acids and their derivatives, Journal of American Chemical Society 94 (1972) 5592–5599.

[28] F. M. Benoit, A. G. Harrison, Predictive value of proton affinity. ionization energy correlations involving oxygenated molecules, Journal of American Chemical Society 99 (1977) 3980–3984.

[29] J. E. Saunders, J. J. Lucier, F. F. Bentley, Far-infrared spectra of saturated esters, Appl. Spectrosc. 22 (6) (1968) 697–713.
URL http://as.osa.org/abstract.cfm?URI=as-22-6-697

[30] A. Vicente, R. Antunes, D. Almeida, I. J. A. Franco, S. V. Hoffmann, N. J. Mason, S. Eden, D. Duflot, S. Canneaux, J. Delwiche, M.-J. Hubin-Franskin, P. Limao-Vieira, Photoabsorption measurements and theoretical calculations of the electronic state spectroscopy of propionic, butyric, and valeric acids, Phys. Chem. Chem. Phys. 11 (2009) 5729–5741. doi:10.1039/B823500G.
URL http://dx.doi.org/10.1039/B823500G